

# Breakdown of a topological phase: Quantum phase transition in a loop gas model with tension

Simon Trebst,<sup>1</sup> Philipp Werner,<sup>2</sup> Matthias Troyer,<sup>3</sup> Kirill Shtengel,<sup>4</sup> and Chetan Nayak<sup>1,5</sup>

<sup>1</sup>Microsoft Research, Station Q, University of California, Santa Barbara, CA 93106

<sup>2</sup>Department of Physics, Columbia University, 538 West 120th Street, New York, NY 10027

<sup>3</sup>Theoretische Physik, Eidgenössische Technische Hochschule Zürich, CH-8093 Zürich, Switzerland

<sup>4</sup>Department of Physics and Astronomy, University of California, Riverside, CA 92521

<sup>5</sup>Department of Physics and Astronomy, University of California, Los Angeles, CA 90095

(Dated: October 6, 2018)

We study the stability of topological order against local perturbations by considering the effect of a magnetic field on a spin model – the toric code – which is in a topological phase. The model can be mapped onto a quantum loop gas where the perturbation introduces a bare loop tension. When the loop tension is small, the topological order survives. When it is large, it drives a continuous quantum phase transition into a magnetic state. The transition can be understood as the condensation of ‘magnetic’ vortices, leading to confinement of the elementary ‘charge’ excitations. We also show how the topological order breaks down when the system is coupled to an Ohmic heat bath and discuss our results in the context of quantum computation applications.

Topological phases are among the most remarkable phenomena in nature. Although the underlying interactions between electrons in a solid are not topologically invariant, their low-energy properties are. This enhanced symmetry makes such phases an attractive platform for quantum computation since it isolates the low-energy degrees of freedom from local perturbations – a usual cause of errors [1]. Tractable theoretical models with topological phases in frustrated magnets [1, 2], Josephson junction arrays [3, 4], or cold atoms in traps [5] have been proposed. However, such phases have not, thus far, been seen experimentally outside of the quantum Hall regime. Is it because topological phases are very rare and these models are adiabatically connected only to very small regions of the phase diagrams of real experimental systems?

In this paper, we take a first step towards answering this question. We begin with the simplest exactly soluble model of a topological phase [1], whose Hamiltonian is given below in Eq. (1). This model describes a frustrated magnet with four-spin interactions similar to cyclic ring exchanges. It is closely related to the quantum dimer model [6] for frustrated magnets, which can be realized in Josephson junction arrays [3]. We consider perturbations of the soluble model that, when sufficiently large, drive the system out of the topological phase. The question is, how large? A small answer would imply that this topological phase is delicate and occupies a small portion of the phase diagram. This might explain the paucity of experimentally-observed topological phases. Instead, we find that ‘sufficiently large’ is a magnetic field  $h$  of order one ( $h_c \approx 0.6$ ) in units of the basic four-spin plaquette interaction. Our numerical simulations demonstrate, for the first time, several key signatures of the phase transition out of the topological phase, including the finite-size degeneracy splitting of the topological sectors, the condensation of ‘magnetic’ excitations, and the confinement of ‘electric’ charges.

We also consider perturbing the system by coupling it to an Ohmic heat bath. When coupled to such a bath, a quantum mechanical degree of freedom can undergo a transition from coherent to incoherent behavior [7]. Recently, the effects of such a coupling on quantum phase transitions, at which di-

vergent numbers of quantum mechanical degrees of freedom interact, have also been studied [8]. In both contexts, the coupling to the heat bath tends to make the system more classical. Coherent quantum oscillations are suppressed, while broken symmetry phases – which are essentially classical – are stabilized. A topological phase is quantum mechanical in nature. We find that coupling the heat bath to the kinetic energy, i.e. plaquette flip operator, does not destroy such a phase. However, when the dissipation is strong, the gap becomes very small, and the topological phase may be too delicate to observe or use at reasonable temperatures. On the other hand, if the heat bath is coupled to the classical state of each plaquette, the topological phase is destroyed through a Kosterlitz-Thouless transition at a dissipation strength of order one.

These results can be recast in quantum information language: the ground states in different topological sectors are the different basis states of an encoded quantum memory. Quasiparticle excitations are states outside of the code subspace. The stability of the topological phase, as measured by an energy gap  $\Delta$  within a topological sector (essentially the energy cost for a pair of quasiparticles), translates into an error rate for topological qubits. At zero temperature, errors are due to the virtual excitation of pairs of quasiparticles, assuming that the system is shielded from perturbations at frequencies higher than  $\Delta$ . Such virtual processes lead to a splitting between topological sectors  $\delta E \sim e^{-\Delta L/v}$ , where  $L$  is the system size and  $v$  is a characteristic velocity. As the temperature is increased, the thermal excitation of particles eventually becomes more important and the error rate is  $\sim e^{-\beta\Delta}$  [25]. (The actual concentration of excitations leading to unrecoverable errors was studied in [10].)

*The model* – We start with the toric code Hamiltonian [1]

$$H_{\text{TC}} = -A \sum_v \prod_{j \in \text{vertex}(v)} \sigma_j^z - B \sum_p \prod_{j \in \text{plaquette}(p)} \sigma_j^x, \quad (1)$$

where the  $\sigma_i$  are  $S = 1/2$  quantum spins on the  $2N$  edges of a square lattice with  $N$  vertices on a torus. Since all terms in Hamiltonian (1) commute with each other, the model can

be solved exactly [1]. The ground-state manifold can be described as a quantum loop gas where the loops consist of chains of up-pointing  $\sigma^z$ -spins and the loop fugacity is  $d = 1$ . On the torus there are four degenerate ground states which can be classified by a winding number parity  $P_{y/x} = \prod_{i \in c_{x/y}} \sigma_i^z$  along a cut  $c_{x/y}$  in the  $x$ - or  $y$ -direction.

Here we study the effect of perturbing the Hamiltonian (1) with a loop tension which can be introduced either by a longitudinal magnetic field or local Ising interaction of the form

$$H = H_{\text{TC}} - h \sum_i \sigma_i^z - J \sum_{\langle ij \rangle} \sigma_i^z \sigma_j^z, \quad (2)$$

where  $h$  ( $J$ ) is the strength of the magnetic field (Ising interaction). These are the dominant perturbations expected in a physical implementation, e.g. in a Josephson junction implementation [3, 4] they arise from electric potential perturbations or Coulomb interactions between neighboring quantum dots. We discuss this model in the limit of a large charge gap, i.e.  $A \gg B, h, J$ , where it becomes equivalent to the ‘even’ Ising gauge theory [11]. The low-energy sector has no free charges and any state is described by a collection of loops that can be obtained from a reference state (e.g. all  $\sigma_i^z = 1/2$ ) by a sequence of plaquette flips. Let us introduce a new plaquette spin operator  $\mu_p$  with eigenvalues  $\mu_p^z = (-1)^{n_p}/2$  where  $n_p$  is the number of times a given plaquette  $p$  has been flipped, counting from the reference state. Then  $\sigma_i^z = 2\mu_p^z \mu_q^z$ , where  $p$  and  $q$  are the plaquettes separated by the edge  $i$ . The plaquette flip term in Eq. (1) becomes  $-4B \sum_p \mu_p^z$ . In the new variables, Hamiltonian (2) becomes equivalent to the transverse field Ising model (with both nearest and next-nearest neighbor Ising interactions) in a basis restricted to loop states. Independent of the choice of basis states the system orders at a critical field strength  $(h/B)_c = 0.65695(2)$  determined by continuous-time quantum Monte Carlo simulations [12]. The transverse field Ising model for the plaquette spins can be mapped to a classical (2+1)-dimensional Ising model:

$$\mathcal{H}_{\text{cl}} = -K_\tau \sum_{\tau, p} S_p(\tau) S_p(\tau + \Delta\tau) - K \sum_{\tau, \langle p, q \rangle} S_p(\tau) S_q(\tau), \quad (3)$$

where the imaginary time  $\tau$  is discretized in steps of  $\Delta\tau$  and  $S_p \equiv 2\mu_p^z = \pm 1$ . The magnetic field  $h$  and the local Ising

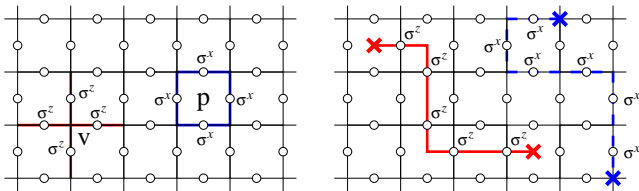


FIG. 1: Left: Illustration of the toric code Hamiltonian (1). Right: The elementary excitations above the loop gas ground state are pairs of ‘magnetic vortices’ on plaquettes connected by a string of  $\sigma^z$ -operators (solid line) and ‘electric charges’ on the vertices connected by a string of  $\sigma^x$ -operators (dashed line).

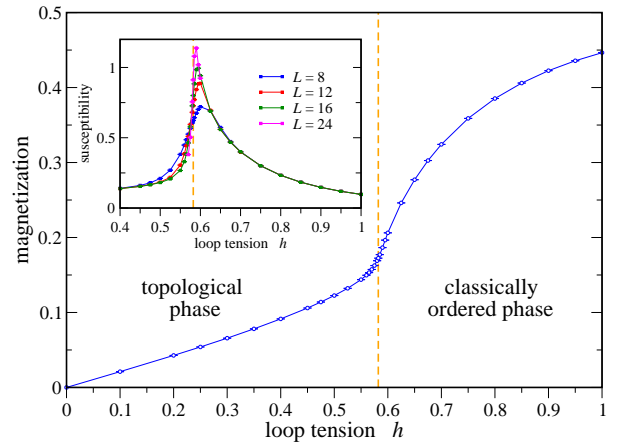


FIG. 2: (Color online) Magnetization  $M = \langle \sum_i \sigma_i^z \rangle / 2N$  versus loop tension (magnetic field). The topological phase survives for small loop tension where an almost constant susceptibility (see inset) leads to a linear increase of  $M$ . Above the critical loop tension (dashed line) the system approaches the fully polarized state.

interaction  $J$  introduce a nearest and next-nearest neighbor interaction between the classical spins  $S_p(\tau)$ , respectively. Since the exact nature of this Ising interaction does not play a role in the following we do not discuss the case of next-nearest neighbor couplings in detail. The coupling along real-space coordinates is then given by  $K = \frac{1}{2} \Delta\tau \cdot h$  and along imaginary time by  $K_\tau = -\frac{1}{2} \ln [\tanh(\Delta\tau \cdot B)]$ . The model (3) describes the well-known continuous magnetic phase transition of the 3D Ising model. For isotropic interactions,  $K = K_\tau$ , the critical coupling has been determined with high precision to be  $K_c = 0.2216595(26)$  [13]. Setting  $B = 1$  this gives a critical loop tension  $h_c = 0.58224$  with isotropic couplings at  $\Delta\tau = 0.761403$ .

The magnetic susceptibility diverges at the transition and

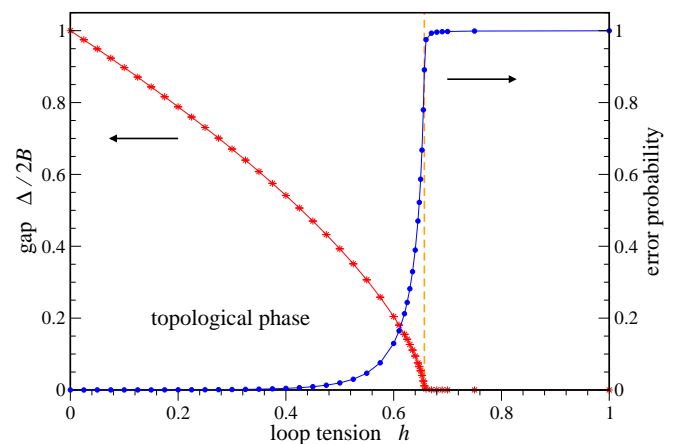


FIG. 3: (Color online) Excitation gap for magnetic vortex excitations (star symbols) versus the loop tension. At the critical loop tension the gap closes and the magnetic vortices condense. Right ordinate: Rate  $\exp(-\beta\Delta)$  for tunneling processes between topological sectors (filled circles) for  $\beta = 10$ .

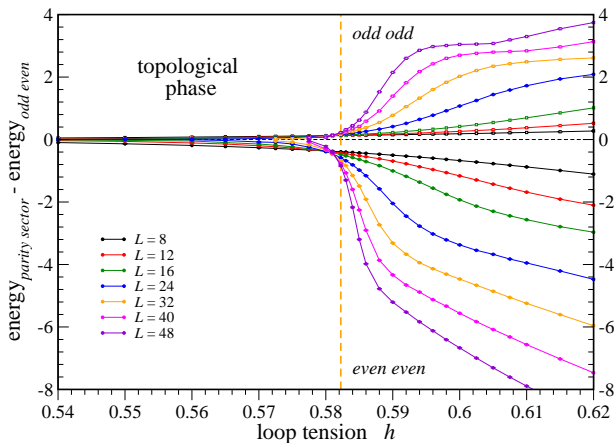


FIG. 4: (Color online) Splitting of the energy degeneracy for the four topological sectors defined by even or odd winding number parities along the  $x$ - and  $y$ -directions. The intermediate {even-odd / odd-even}-parity sector was taken as a reference (dashed line).

the magnetization  $\langle \sum_i \sigma_i^z \rangle / 2N$  shows a corresponding kink, as shown in Fig. 2. Although this is not a symmetry-breaking transition, the analogous transition driven by next-nearest interaction  $J$  is a *continuous* quantum phase transition from a topologically ordered quantum state to a broken symmetry state [14]. The magnetic transition can also be understood in terms of the condensation of ‘magnetic vortices’, plaquettes with  $\prod_j \sigma_j^x = -1$ . While for the original Hamiltonian (1), the gap to these excitations is  $\Delta = 2B$ , they become gapless and condense at the critical loop tension, as shown in Fig. 3. The gap has been estimated from measurements of the imaginary time correlation length  $\xi_\tau$  as  $\Delta \propto 1/\xi_\tau$  which we have calculated applying continuous-time quantum Monte Carlo simulations using the ALPS looper code [15, 16]). The thermal excitation of pairs of magnetic vortices occurs with probability  $\sim \exp(-\beta\Delta)$ , also shown in Fig. 3.

*Topological order* – The breakdown of topological order at the phase transition can be seen from the energy splitting  $\delta E$  between the ground-states for the various topological sectors. When winding parities are used as basis states for a quantum memory, this splitting causes phase errors. (The absence of ‘electric’ charges precludes any transitions between different winding parities so bit flip errors cannot occur.) In the topological phase, the virtual excitation of quasiparticles leads to a small splitting  $\delta E \propto \exp(-\Delta L/v)$  between the topological sectors. In the classically-ordered phase, on the other hand, the energy splitting should scale with  $L$ , which corresponds to the energy cost of a loop in the ordered ground state. As the winding parity is conserved by imaginary time spin-flip operations, we can simulate the system in one of the topological sectors by defining an initial spin configuration that corresponds to the respective limit for large loop tension. Fig. 4 shows the calculated splitting for various system sizes in the vicinity of the critical loop tension. At the phase transition, the behavior qualitatively changes from power-law scaling for strong loop tension to an exponential suppres-

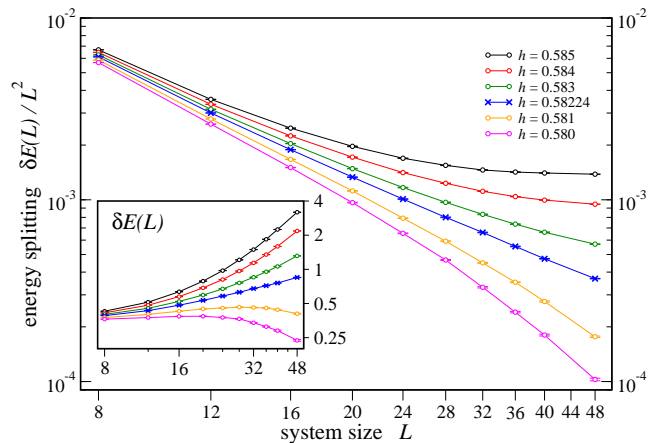


FIG. 5: (Color online) Finite-size scaling of the energy splitting between the topological sectors around the quantum phase transition for  $\beta = 10L$ . At the critical loop tension (crosses) we find power-law scaling  $\delta E(L) \propto L^{2-z}$  with exponent  $z = 1.42 \pm 0.02$ .

sion in the topological phase for small loop tension as discussed above. A more quantitative picture arises from the finite-size scaling analysis of the energy splitting  $\delta E(L)$  between the {even-odd}- and {even-even}-parity sectors shown in Fig. 5. For the critical loop tension we find a power-law scaling  $\delta E(L) \propto L^{2-z}$  with an exponent  $z = 1.42 \pm 0.02$ . Below the critical value the scaling turns into exponential scaling as expected for the topological phase.

*Confinement transition* – For the loop gas Hamiltonian (1) the elementary electric charge excitations (end-points of an open loop) are deconfined. For strong loop tension, however these excitations are expected to become confined, thereby eliminating all open loops. We can study this confinement transition in our simulations of model (3) by artificially introducing pairs of electric charge excitations for the sampled loop configurations. This allows us to measure the confinement length  $\xi_c$  as the square root of the average second moment of the distance between the two excitations, which for a torus with even extent  $L$  has to be normalized by a factor  $6/(L^2 + 2)$ . The measured confinement length  $\xi_c$  shown in Fig. 6 clearly demonstrates that electric charges remain deconfined for the full extent of the topological phase and that the confinement transitions occurs simultaneously with the magnetic phase transition. At the critical loop tension the confinement lengths  $\xi_c(L)$  for various system sizes cross which demonstrates that the confinement length diverges with the *same* critical exponents as the magnetic correlation length  $\xi$  and there is only one length scale describing the phase transition. This can be seen from the following finite-size scaling argument: We may write the finite-size scaling behavior for the confinement length as  $\xi_c(\tau, L) \propto \tau^{-\nu} f(L\tau^\chi)$  where  $\nu$  ( $\chi$ ) is the critical exponent of the correlation (confinement) length respectively and  $\tau = h - h_c$ . With  $\tilde{f}(L^{1/\chi}\tau) = (L^{1/\chi}\tau)^{-\nu} f(L\tau^\chi)$  we obtain for the confinement length  $\xi_c(\tau, L) \propto L^{\nu/\chi} \tilde{f}(L^{1/\chi}\tau)$ . At the phase transition the existence of a crossing point  $\xi_c(0, L)/L \propto$

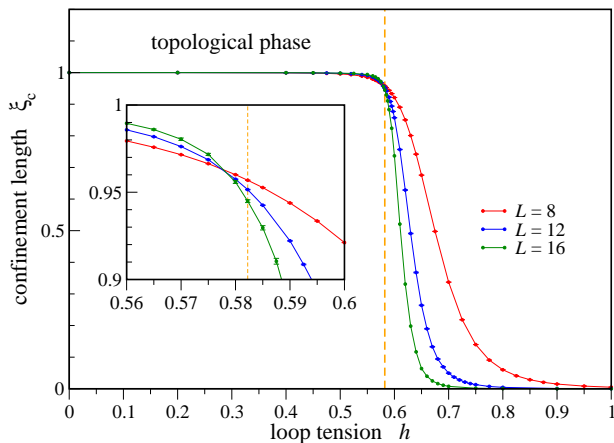


FIG. 6: (Color online) Confinement length of two electric charge excitations versus loop tension. The confinement transition occurs at the same critical loop tension (dashed line) as the magnetic transition.

$L^{\nu/\chi-1} = \text{const}$  then implies  $\chi = \nu$ . For our model without dynamical electric charges, this measure of the confinement of test charges is closely related to the calculation of a Wilson loop expectation value. In the presence of dynamical electric charges, this becomes trickier; Polyakov loops have been used as an order parameter for the *finite* temperature transition of the 3D Ising gauge model[17].

*Dissipation* – Finally, we discuss the effect of dissipation when Hamiltonian (1) is coupled to an Ohmic heat bath. Since our model excludes dynamical electric charges, we do not consider coupling a heat bath directly to  $\sigma_i^x$ . Instead, we first examine coupling a heat bath to  $\mu_p^x$  so that a ‘phonon’ is created when a plaquette flips. This type of dissipation could occur in a Josephson junction model [18] or in a spin model through the spin-phonon coupling. The standard procedure [19] for a linear spectral density (‘Ohmic’ dissipation) results in an effective action for independent Ising chains with long-range couplings in an external *longitudinal* magnetic field (which here means parallel to  $\mu^x$ ). We note that as a consequence of the Lee–Yang theorem [20], there can be *no singularities* of the respective partition function at any real non-zero longitudinal field, ruling out the existence of a quantum phase transition for this model. In particular, this implies that the magnetic gap remains finite for any dissipation strength!

An entirely different behavior arises if dissipation is coupled such that it stabilizes the ‘classical’ state of the system. Coupling the bath to either  $\sigma_i^z$  or  $\mu_p^z$  stabilizes the classical state of a single spin or a plaquette, respectively. We consider the latter as it should be more effective at damping quantum fluctuations, although we expect the former to have similar physics. The same procedure as above then leads to a model

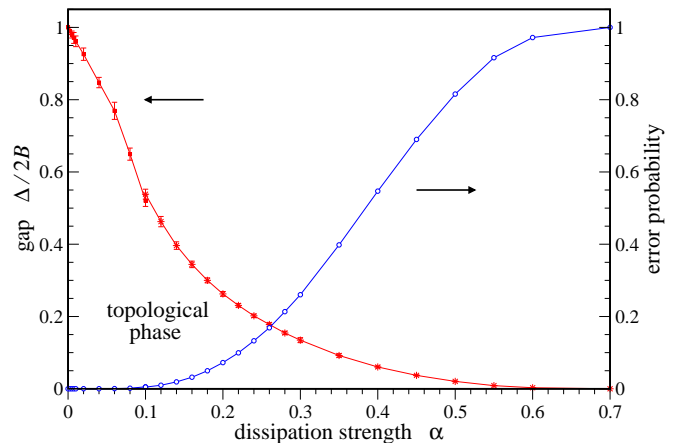


FIG. 7: (Color online) Gap and error probability versus dissipation strength estimated from the correlation time  $\xi_\tau$  of the dissipative Ising chain (4).

for decoupled Ising chains given by

$$\mathcal{H}_{\text{cl}} = -K_\tau \sum_{\tau,p} S_p(\tau) S_p(\tau + \Delta\tau) - \frac{\alpha}{2} \sum_{\tau < \tau',p} \left( \frac{\pi}{N_\tau} \right)^2 \frac{S_p(\tau) S_p(\tau')}{\sin^2\left(\frac{\pi}{N_\tau} |\tau - \tau'|\right)}, \quad (4)$$

where the parameter  $\alpha$  measures the dissipation strength. This model has been well studied [21] and is known to exhibit a Thouless-type phase transition into a classically disordered, fluctuationless phase. The critical value  $\alpha_c$  of this transition depends weakly on the cutoff in the long-range interaction; in our simulations  $\alpha_c \approx 0.7$ . At the transition the magnetic gap vanishes, in sharp contrast to the previous case.

Due to the long range interactions introduced by the dissipative coupling, the spin-spin correlations will asymptotically decay as  $1/\tau^2$  [22]. It is therefore a non-trivial task to define a correlation-time and hence to estimate the excitation gap. For  $\alpha \lesssim 0.1$  one observes an exponential decay of the correlation function onto the asymptotic  $1/\tau^2$  behavior, and subtracting the  $1/\tau^2$ -contribution allows one to estimate  $\xi_\tau$ , which is found to grow linearly with  $\alpha$ . For  $\alpha > 0.1$ , this procedure can no longer be used. In this region we estimate  $\xi_\tau$  from the asymptotic decay of the correlations, proportional to  $(\xi_\tau/\tau)^2$ . These  $\xi_\tau$ s grow approximately exponentially in the region  $0.1 \lesssim \alpha \lesssim \alpha_c$ . Alternatively, one could define a correlation-time from the crossover scale where the short-time behavior crosses over to the asymptotic  $1/\tau^2$  form. This definition in the spirit of a ‘Josephson length’ [23] yields (up to a normalization factor) the same results as the  $\xi_\tau$  extracted from the asymptotic decay. The gap estimated from the inverse correlation function, as well as the error probability is plotted in Fig. 7. We find that the error probability remains negligibly small below the crossover value  $\alpha \approx 0.1$ .

*Outlook* – We have shown that the topological phase which governs the toric code model [1] actually exists in an extended region of phase space around the soluble point. It

is stable against deviations of the system Hamiltonian from the ideal one and also the coupling of the system to its environment. In general, this demonstrates that a system does not necessarily have to be particularly fine-tuned to reach a topological phase. The paucity of their experimental observations may thus be due not to some intrinsic delicateness of such phases, but rather to the experimental subtlety involved in identifying them. In future work, these conclusions need to be tested in other, more exotic topological phases which support universal topological quantum computation [24].

We thank E. Ardonne, L. Balents, S. Chakravarty, and A. Kitaev for stimulating discussions.

- 
- [1] A. Yu. Kitaev, *Ann. Phys.* **303**, 2 (2003).  
 [2] R. Moessner and S. L. Sondhi, *Phys. Rev. Lett.* **86**, 1881 (2001); C. Nayak and K. Shtengel, *Phys. Rev. B* **64**, 064422 (2001); L. Balents, M. P. A. Fisher, and S. Girvin, *Phys. Rev. B* **65**, 224412 (2002); M. Freedman, *et al.* *Ann. Phys.* **310**, 428 (2004); M. A. Levin and X.-G. Wen, *Phys. Rev. B* **71**, 045110 (2005); P. Fendley and E. Fradkin, *Phys. Rev. B* **72**, 024412 (2005).  
 [3] L. B. Ioffe *et al.*, *Nature* **415**, 503 (2002).  
 [4] O. I. Motrunich and T. Senthil, *Phys. Rev. Lett.* **89**, 277004 (2002).  
 [5] L.-M. Duan, E. Demler, and M. D. Lukin, *Phys. Rev. Lett.* **91**, 090402 (2003); V. Gurarie, L. Radzihovsky, and A. V. Andreev, *Phys. Rev. Lett.* **94**, 230403 (2005).  
 [6] D. S. Rokhsar and S. A. Kivelson, *Phys. Rev. Lett.* **61**, 2376 (1988).  
 [7] A. Leggett *et al.*, *Rev. Mod. Phys.* **59**, 1 (1987).  
 [8] P. Werner *et al.*, *Phys. Rev. Lett.* **94**, 047201 (2005); P. Werner *et al.*, *J. Phys. Soc. Jpn. Suppl.* **74**, 67 (2005).  
 [9] C. Chamon, *Phys. Rev. Lett.* **94**, 040402 (2005).  
 [10] C. Wang, J. Harrington, and J. Preskill, *Ann. Phys.* **303**, 31 (2003).  
 [11] R. Moessner, S. L. Sondhi, and E. Fradkin, *Phys. Rev. B* **65**, 024504 (2002).  
 [12] H. W. J. Blöte and Y. Deng, *Phys. Rev. E* **66**, 066110 (2002).  
 [13] A. M. Ferrenberg and D. P. Landau, *Phys. Rev. B* **44**, 5081 (1991).  
 [14] E. Ardonne, P. Fendley, and E. Fradkin, *Ann. Phys.* **310**, 493 (2004).  
 [15] F. Alet *et al.*, *J. Phys. Soc. Jpn. Suppl.* **74**, 30 (2005). See also <http://alps.comp-phys.org>.  
 [16] S. Todo and K. Kato, *Phys. Rev. Lett.* **87**, 047203 (2001).  
 [17] M. Caselle, M. Hasenbusch, and M. Panero, *JHEP* **01**, 057 (2003).  
 [18] G. Schön and A. D. Zaikin, *Phys. Rep.* **198**, 237 (1990).  
 [19] A. O. Caldeira and A. J. Leggett, *Ann. Phys.* **149** 374 (1983).  
 [20] T. D. Lee and C. N. Yang, *Phys. Rev.* **87**, 410 (1952).  
 [21] D. J. Thouless, *Phys. Rev.* **187**, 732 (1969); J. Fröhlich and T. Spencer, *Commun. Math. Phys.* **84**, 87 (1982); J. Bhattacharjee *et al.*, *Phys. Rev. B* **24**, 3862 (1981); E. Luijten and H. Messingfeld, *Phys. Rev. Lett.* **86**, 5305 (2001).  
 [22] R. B. Griffiths, *J. Math. Phys.* **8**, 478 (1967).  
 [23] S. Chakravarty and J. Rudnick, *Phys. Rev. Lett.* **75** 501 (1995).  
 [24] M. H. Freedman, *Found. Comput. Math.* **1**, 183 (2001), and references therein.  
 [25] In a special case of a topological phase considered in [9], thermal activation *always* dominates quantum tunneling.